Molecular Crystals and Liquid Crystals
Publication details, including instructions for authors and subscription information:
http://www.tandfonline.com/loi/gmcl16

Macroscopic Properties of Liquid Crystals

Michael G. Clark [a]

[a] Optical and Display Science Division, Royal Signals and Radar Establishment, Malvern, Worcestershire, WR14 3PS, UK

Version of record first published: 17 Oct 2011.

To cite this article: Michael G. Clark (1985): Macroscopic Properties of Liquid Crystals, Molecular Crystals and Liquid Crystals, 127:1, 1-41

To link to this article: http://dx.doi.org/10.1080/00268948508080829

Mol. Cryst. Liq. Cryst., 1985, Vol. 127, pp. 1–41
0026-8941/85/1274–0001/$30.00/0

Printed in the United States of America

Macroscopic Properties of Liquid Crystals†

MICHAEL G. CLARK

Optical and Display Science Division, Royal Signals and Radar Establishment, Malvern, Worcestershire, WR14 3PS, UK

(*Received November 22, 1984*)

The macroscopic properties of nematic liquid crystals relevant to device performance are discussed from both continuum and molecular points of view. Key concepts and points of difficulty are emphasized, and some areas in greatest need of further work are identified.

1. DEFINITIONS AND MOTIVATION

The macroscopic properties of liquid crystals are those properties which can be described in terms of continuum theory. However, since their origin can only be understood in molecular terms they form a bridge between the device physics of LCDs and the materials science of liquid crystals. Thus the operation of an LCD can be described by specifying the spatial and time dependence of the director $\mathbf{n}(\mathbf{r}, t)$ and the fluid velocity $\mathbf{v}(\mathbf{r}, t)$. Both of these are continuum variables. The time-independent "statics" of LCDs involves consideration of the equilibrium director configurations $\mathbf{n}(\mathbf{r})$ and their optical properties. These depend on macroscopic properties such as the electric permittivity, refractive indices, absorption coefficients, and orientational elastic constants. The time-dependent "dynamics" depends in addition on macroscopic properties such as conductivity and viscosity. Since these are all continuum quantities, in order to understand liquid crystal *devices* it is *not* necessary to consider explicitly the molecules

†Plenary Lecture presented at the 10th International Liquid Crystal Conference, York, July 15th–21st, 1984.

of which the liquid crystal is composed. However, as will be emphasized below, the macroscopic properties are determined by the molecular and fluid structure of the liquid. Thus in order to understand liquid crystal *materials* it is essential to consider molecular theories.

Understanding and measurements of macroscopic properties are needed both to enable device physicists to model and predict device performance, and to stimulate predictive theories relating macroscopic properties to molecular and fluid structure, thus offering a less empirical approach to the molecular engineering of liquid crystal materials. In this paper these matters are reviewed mainly in the context of nematics, but with some reference to the properties of smectic A materials.

1.1. The director

This quantity is most simply and unambiguously defined in continuum terms. A nematic liquid has local uniaxial symmetry: the director $\mathbf{n}(\mathbf{r}, t)$ is a unit vector parallel to this symmetry axis. Since the phase is centrosymmetric $\mathbf{n}$ and $-\mathbf{n}$ are equivalent.

The definition of the director in molecular terms encounters rather greater difficulties. Often it is said that the director is the average preferred direction (unsigned since $\mathbf{n}$ is equivalent to $-\mathbf{n}$) of the molecules. This average must be taken over a sample of fluid sufficiently large for the average to be independent of the size and shape of the sample; since the largest linear dimension of nematic molecules is typically a few nm a sample size of say $(0.1\ \mu\text{m})^3$ should be more than sufficient. The minimum sample size presumably sets one lower limit on the applicability of continuum theory. A more serious difficulty, as we shall see, is that of defining precisely what is meant by the preferred direction of a molecule.

One point which is clarified by discussion of the direction in molecular terms is that the director and the "molecular orientation" are different things. A consequence of thermal motions is that, to put it simply, the molecules are jumbled but the director is not—or at least (see Sec. 4.3) not very much.

1.2. Molecular order parameters

The extent to which the molecules are jumbled is quantified by the molecular order parameters. Cartesian axes (X', Y', Z') fixed in a particular molecule are related to the laboratory frame (X, Y, Z), in which we take Z parallel to $\mathbf{n}$, by Euler angles[1] (ϕ, θ, ψ) as illustrated in Figure 1. The single-molecule orientational distribution function

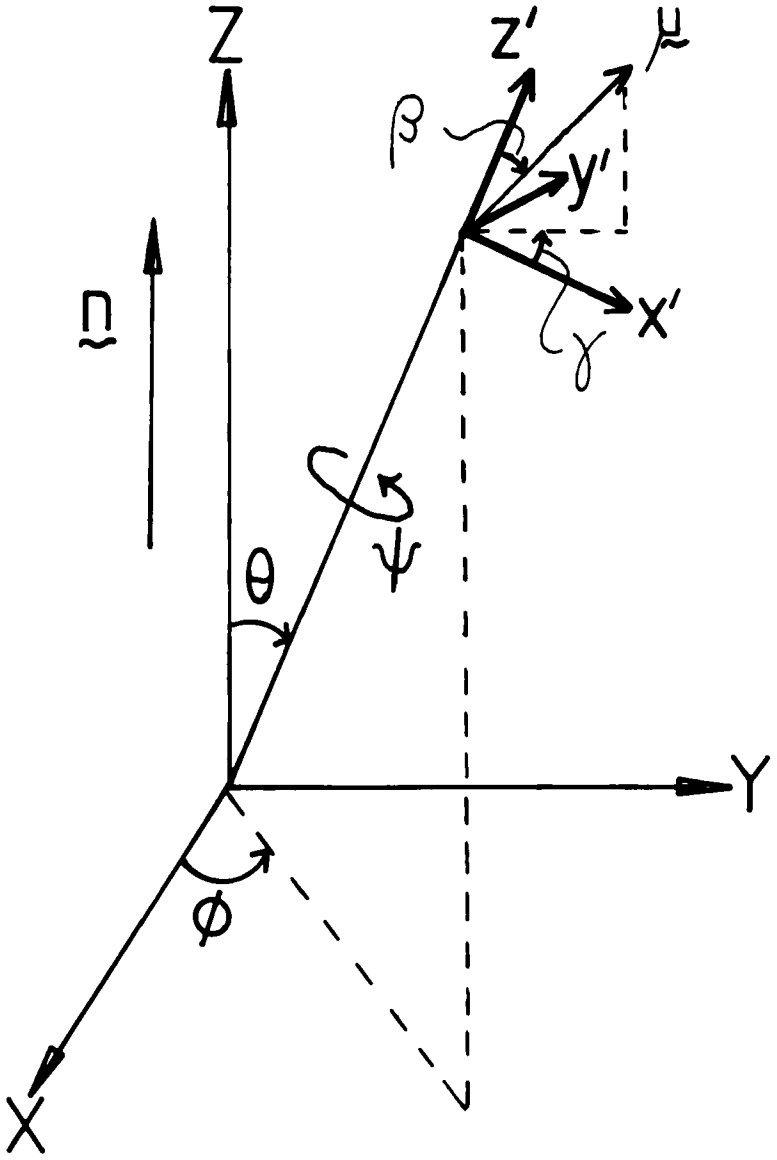

FIGURE 1 Definitions of axes and angles used in the text.

$f(\phi, \theta, \psi)$ describes the statistical distribution of molecular orientations due to thermal motion. It is constrained by the symmetry of the nematic phase to be independent of ϕ. Thus it can be expanded in terms of the modified spherical harmonics[1] $C_{lm}(\theta, \psi)$ to give

$$f(\theta, \psi) = \frac{1}{4\pi} \sum_{l,m \text{ even}} (2l + 1) S_{lm} C_{lm}(\theta, \psi) \tag{1.1}$$

where

$$S_{lm} = \int f(\theta, \psi) C_{lm}^*(\theta, \psi) \sin\theta d\theta d\psi \tag{1.2}$$

are the molecular order parameters. The nematic phase being uniaxial and centrosymmetric, l and m must be even and S_{lm} real. The second of these conditions means that for $m \neq 0$ it is convenient to use the real parameters

$$S^c_{l|m|} = (2)^{-1/2}(S_{l-m} + S^*_{l-m}) \tag{1.3}$$

$$S^s_{l|m|} = i(2)^{-1/2}(S_{l-m} - S^*_{l-m}) \tag{1.4}$$

Thus the lowest order non-vanishing S_{lm} belong to $l = 2$:

$$m = 0 \quad \langle \tfrac{1}{2}(3\cos^2\theta - 1) \rangle = S \quad \text{"order parameter"} \tag{1.5}$$

$$|m| = 2 \quad \langle \tfrac{1}{2}\sqrt{3}\sin^2\theta \cos 2\psi \rangle = D \text{ "biaxiality parameter"} \tag{1.6}$$

Many of the properties of greatest device interest depend only on these two order parameters, and there has consequently been relatively little discussion in the literature of higher order S_{lm}. Indeed, as reflected by its appellation as "the order parameter," most workers have considered only the S_{20} parameter S. However, it is becoming increasingly clear that D, which measures asymmetry in the single-molecular distribution function, is non-zero in typical nematics[2] and may become quite large for plate-like molecules (anthraquinone dyes) in nematic solution.[3] Note that there is no consensus in the literature on the normalization of D, with at least two alternative numerical pre-factors in use instead of the $\frac{1}{2}\sqrt{3}$ used in Eq. (1.6). Observe also that we have neglected the complication of molecular flexibility.[4,5]

We remark in passing that the "optical order parameter"

$$S_{op} = (A_\parallel - A_\perp)/(A_\parallel + 2A_\perp) \tag{1.7}$$

where $A_\parallel$, $A_\perp$ are absorbances for light polarized parallel and perpendicular to the nematic director, is simply a rearrangement of the

macroscopic parameters $A_{\parallel}$, $A_{\perp}$ and is therefore itself a macroscopic parameter, not a molecular order parameter.

1.3. Other phases

The symmetry of the nematic phase may be modified in various ways to give other liquid crystal phases. We consider only the most familiar; the cholesteric and smectic A phases.

In the cholesteric phase the modification, although stemming from molecular chirality, is essentially at a continuum level with the director adopting a helical configuration with pitch of order μm, i.e. of length scale at which continuum theories are applicable. As far as can be determined, in thermotropic liquid crystals the material remains locally uniaxial and nematic-like. Thus, with the obvious exception of properties relating directly to the helical twist or molecular chirality, the macroscopic properties are much the same as those of a nematic.

In the case of a smectic A, a mass density wave

$$\rho(z) = \rho_0[1 + \sqrt{2}|\psi_s|\cos(q_s z - \phi_s)] \tag{1.8}$$

with complex order parameter

$$\psi_s = |\psi_s|\exp(i\phi_s) \tag{1.9}$$

is superposed parallel to **n** on the nematic order. The modification here is at a molecular level with the wavelength of the density wave $2\pi/q_s$ being of the order of one or two molecular lengths.[6] Reflecting this, certain of the macroscopic properties of nematics are strongly influenced by the juxtaposition of a real or incipient smectic A phase. This we discuss in greater detail below, with the motivation that such effects can be employed in the molecular engineering of nematic properties.

1.4. Phenomenology

The macroscopic properties determine the strengths of physical effects occurring in liquid crystals. Such effects may be electro-optic, thermo-optic, magneto-optic, etc. As summarized in Figure 2, an effect must be simultaneously considered as a candidate for device application, as a probe of device physics, and (most importantly for the present paper) as a method for measurement of one or more of the macroscopic properties which determine its strength.

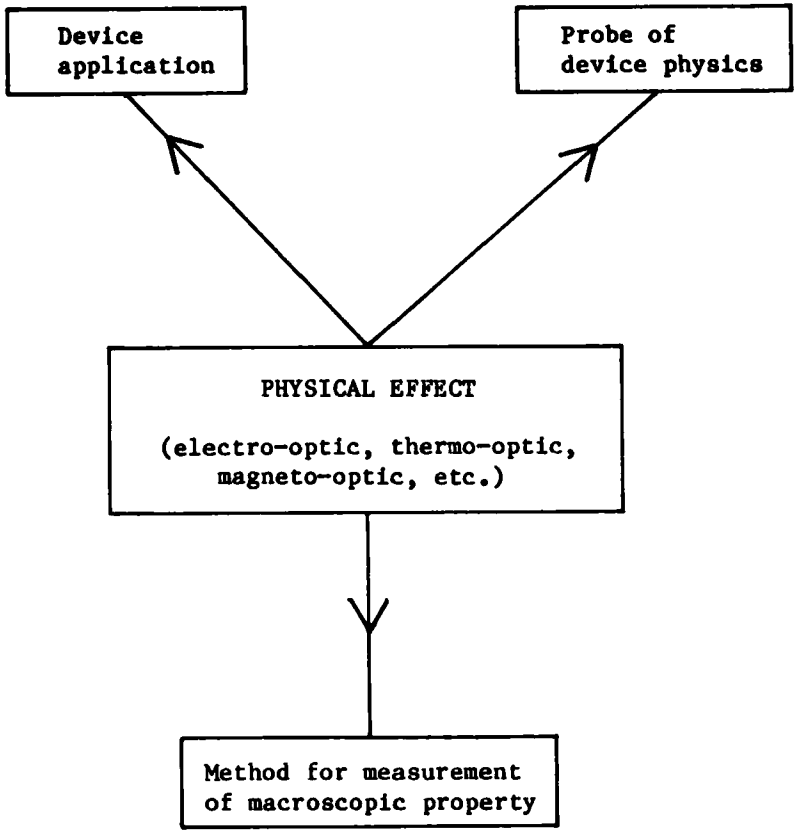

FIGURE 2 The implications of a physical effect.

Measurement of the macroscopic properties of liquid crystal materials is essential both for molecular engineering of their properties and as a data base for device modelling. Table I summarizes some of the features desired in methods for routine measurement of macroscopic properties. Many of the features are almost self-evident. Applicability to small samples is an important feature since newly synthesized organic materials are rarely available in large quantities. It is highly desirable that measurement methods should be applicable over the full range of relevant macroscopic parameters, and essential that a sound and accurate quantitative theoretical description of the experiment be available if unsuspected systematic errors are to be avoided.

TABLE I

Some features desired in methods for routine measurement of macroscopic properties

Rapid, accurate, precise
Small sample (<0.1 g)
Readily automated
Low capital cost
Unrestricted applicability
Good theory

2. ANISOTROPIC PROPERTY TENSORS

Many of the most important macroscopic properties can be classified as *property tensors* since they describe multi-linear relationships between tensor influences and effects. For example the permittivity tensor describes the dipole moment density (polarization) induced in a material by application of an electric field **E**. The linear relationship between polarization and field is a familiar one:

$$\mathbf{P} = \epsilon_0(\boldsymbol{\epsilon} - \mathbf{I})\mathbf{E} \tag{2.1}$$

or in Cartesian component notation

$$P_i = \epsilon_0(\epsilon_{ij} - \delta_{ij})E_j \tag{2.2}$$

The permittivity tensor is an example of a Cartesian second-rank (two indices) property tensor. In the axially-symmetric nematic phase such tensors may be specified by principal axes parallel and perpendicular to the director **n**, and corresponding principal values for a tensor **T** of $T_\parallel$ and $T_\perp$. Thus, in arbitrary axes

$$T_{ij} = \tfrac{1}{3}(T_\parallel + 2T_\perp)\delta_{ij} + (T_\parallel - T_\perp)(n_i n_j - \tfrac{1}{3}\delta_{ij}) \tag{2.3}$$

$$= T_\perp \delta_{ij} + (T_\parallel - T_\perp)n_i n_j \tag{2.4}$$

The linear combinations of $T_\parallel$ and $T_\perp$ used on the right-hand side of Eq. (2.3) are usefully identified as separate quantities of physical interest:

$$\tfrac{1}{3}(T_\parallel + 2T_\perp) = \overline{T} \qquad \text{"spherical mean"} \tag{2.5}$$

$$T_\parallel - T_\perp = \Delta T \qquad \text{"anisotropy"} \tag{2.6}$$

In general the relationship between macroscopic property tensors and molecular property tensors is a complex one, but for a few properties, e.g. magnetic susceptibility, the macroscopic tensor may usefully be approximated as a thermally-averaged sum of the molecular tensor. The relationship is then a simple linear one involving the molecular order parameters, Sec. 1.2, and is most elegantly written in spherical tensor notation:[1]

$$T_{kq} = \delta_{q0} 2\pi \sum_p t_{kp} S_{kp} \tag{2.7}$$

where t_{kp} is the corresponding molecular tensor and, as noted in Sec. 1.2, the order parameters S_{kp} have k, p even and are real.

3. PERMITTIVITY

3.1. "Static" ϵ

The simplest viable theory of nematic permittivities is that of Maier and Meier,[7] which gives

$$\epsilon_{\parallel} = 1 + (NhF/\epsilon_0)\{\bar{\alpha} + \tfrac{2}{3}S\Delta\alpha + (F/3k_BT)[\mu_l^2(1 + 2S) + \mu_t^2(1 - S)]\} \tag{3.1}$$

$$\epsilon_{\perp} = 1 + (NhF/\epsilon_0)\{\bar{\alpha} - \tfrac{1}{3}S\Delta\alpha + (F/3k_BT)[\mu_l^2(1 - S) + \mu_t^2(1 + \tfrac{1}{2}S)]\} \tag{3.2}$$

where (see Figure 1) μ_l and μ_t are the components of the molecular electric dipole moment longitudinal and transverse to the "long axis" Z' of the molecule,

$$\mu_l = \mu\cos\beta \qquad \mu_t = \mu\sin\beta \tag{3.3}$$

$\bar{\alpha}$ and $\Delta\alpha$ are the spherical mean and anisotropy of the molecular polarisability [cf. Eqs. (2.5) and (2.6)], the quantities

$$h = 3\bar{\epsilon}/(2\bar{\epsilon} + 1) \tag{3.4}$$

$$F = 1/(1 - \bar{\alpha}f) \tag{3.5}$$

$$f = (2N/3\epsilon_0)[(\bar{\epsilon} - 1)/(2\bar{\epsilon} + 1)] \tag{3.6}$$

are internal field factors, and N is the number density of molecules. In Eqs. (3.1) and (3.2) ϵ is expressed as a sum of contributions from molecular polarizability and molecular dipole. As emphasized in Sec. 2 it is convenient to consider $\Delta\epsilon$ and $\bar{\epsilon}$ separately as they reflect physically distinct aspects.

The anisotropy $\Delta\epsilon$ is of particular importance in determining the response of the nematic in electric field induced electro-optic effects. There are requirements for both positive and negative $\Delta\epsilon$ materials. From Eqs. (3.1) and (3.2):

$$\Delta\epsilon = (NhF/\epsilon_0)[\Delta\alpha + (F/k_BT)(\mu_l^2 - \tfrac{1}{2}\mu_t^2)]S \qquad (3.7)$$

The contribution from anisotropy of the molecular polarizability is quite small compared with that potentially available from the molecular dipole. Thus the molecular engineering of $\Delta\epsilon$ is concentrated on the dipolar contribution. From Eq. (3.7) it is clear that μ_t is 50% less efficient at generating negative $\Delta\epsilon$ than μ_l is at generating positive $\Delta\epsilon$. Thus in Table II we compare data taken from the literature[8] on positive and negative materials with similar dipole moments (roughly 15×10^{-30} C m). Neglecting variations in the polarizability contribution, and in the number density N and internal field factors, the quantity $T\Delta\epsilon$ at a fixed reduced temperature (T/T_c where T_c is the absolute N to I transition temperature) is a rough measure of the dipolar contribution to $\Delta\epsilon$.

The needs of the twisted nematic LCD have stimulated the development of materials with positive $\Delta\epsilon$. From Eq. (3.7) the desired conditions are μ_l large and $\mu_t \sim 0$. These are met by use of polar terminal substituents, of which the CN group has been the dominant

TABLE II

Comparison of positive and negative $\Delta\epsilon$ nematics with similar dipole moments[8] (roughly 15×10^{-30} C m)

	$10^{-3}T\Delta\epsilon$ $(0.95T_c)$
	5.85
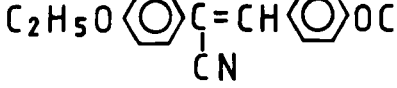	−1.65

example. Table III lists examples of the main families that have been developed. Also shown are values for the molecular electric dipole moment μ and the quantity $T\Delta\epsilon$ at $0.95T_c$.[9] If the dipole moment is parallel to the "long axis" ($\beta = 0$) and if, as assumed in Maier-Meier theory, the only significant intermolecular correlation is the long range nematic order, then $T\Delta\epsilon$ and μ should be correlated, with $T\Delta\epsilon$ roughly proportional to μ^2. The figures in the rightmost column of Table III, which have been corrected for variations in number density but not for the polarizability contribution, indicate clearly that the situation is more complex. Whether or not the "long axis" makes a significantly non-zero angle with the molecular dipole in any of the materials listed in Table III is a matter for debate, but, as discussed below, there is clear evidence of local intermolecular correlations significantly modifying macroscopic properties in some materials.

TABLE III

Examples of the main families of positive $\Delta\epsilon$ nematics[9]

	μ 10^{-30} C m	$10^{-3}T\Delta\epsilon$ $(0.96T_c)$	$\frac{10^{-57}N_A T\Delta\epsilon}{N\mu^2}$
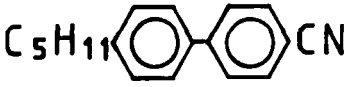	16.0	4.09	~4
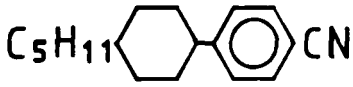	13.8	3.36	4.76
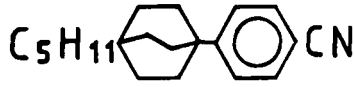	13.6	3.50*	5.45
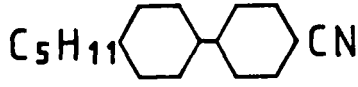	12.0	1.49	2.96
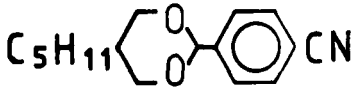	23.0	4.88*	2.50
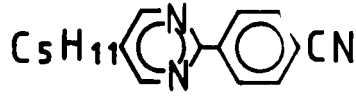	22.0	7.38	3.76

* mixture of propyl/pentyl/heptyl homologues

Before turning to this question, the situation concerning materials with negative $\Delta\epsilon$ must be considered. This is altogether less satisfactory. The requirement for $\mu_l \sim 0$ and μ_t large implies polar lateral substituents which have tended to create problems such as difficult syntheses, chemical instability, and high viscosity. Table IV lists a few of the structures which have been considered, together with limited representative data.[10,11,12] The bicyclohexyl-β-carbonitriles[12] (IV in Table IV) and related compounds should be highlighted as perhaps the most promising and ingenious approach.

Whereas the anisotropy $\Delta\epsilon$ is proportional to S, the mean permittivity $\bar{\epsilon}$ is essentially free from order parameter effects, and thus is a sensitive test of local molecular correlations. From Maier-Meier theory one gets

$$\bar{\epsilon} = 1 + (NhF/\epsilon_0)[\bar{\alpha} + (F/3k_BT)\mu^2] \tag{3.8}$$

TABLE IV

Some examples of negative $\Delta\epsilon$ nematics[10,11,12]

(I) 	$\Delta\epsilon = -22$
(II) 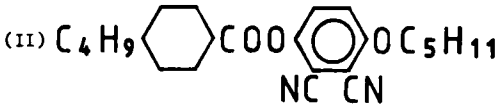	$\Delta\epsilon = -17$
(III) 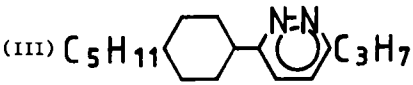	$\Delta\epsilon = -8.3$
	4°C $0.97T_c$
(IV) 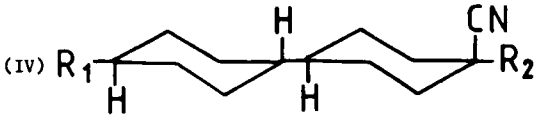	$\Delta\epsilon = -10$
	20°C $0.88T_c$

which predicts a continuous temperature variation of $\bar{\epsilon}$ through the nematic to isotropic transition, with $\partial\bar{\epsilon}/\partial T$ negative. Such a variation is seen in some materials, e.g. 4,4′-dialkylphenylbenzoates R · C_6H_4 · COO · C_6H_4 · R′, whereas in CN-terminated materials such as the alkyl cyanobiphenyls $\bar{\epsilon}$ shows a discontinuity at T_c and a strong pretransitional effect, both associated with the "antiparallel" local molecular correlations which occur in these materials. These effects are graphically illustrated by adding 4-*n*-propyl-4′-*n*-heptylphenylbenzoate (Me37) to 1-(4′-cyanophenyl)4-*n*-propylbicyclo(2,2,2)octane (3BCO).[13] As shown in Figure 3, both the discontinuity and the pretransitional effect disappear as the antiparallel correlations of nearest-neighbour 3BCO molecules are broken up by addition of the ester.

3.2. Molecular engineering vs fluid engineering

The process of optimising the macroscopic properties of a liquid crystal material for a particular application is an example of what is loosely termed "molecular engineering." In reality both the molecular structure, i.e. the atoms present and the chemical bonds between them, and the fluid strucure, i.e. the packing and thermal motions of the molecules, must be engineered. As summarized in Table V the evidence, of which Sec. 3.1 cites examples, is clearly that the macroscopic property ϵ may be strongly influenced by the fluid structure. For example, anti-parallel nearest-neighbour correlations are to a lesser or greater extent a significant feature in all the nematic fluids listed in Table III.

Another important corollary of this line of reasoning is that the macroscopic properties of a neat nematic liquid may be a poor guide to the contribution which molecules of that liquid would make to the macroscopic properties of a mixture. In the case of static permittivity one could argue from Table V that the molecular properties μ and, perhaps, β may be better guides to the dopant behaviour than the macroscopic property ϵ of the neat liquid.

3.3. Dielectric relaxation

The "static" permittivity describes the polarization induced in the material by an external electric field whose frequency of alternation is sufficiently low for the perturbations induced in the molecular dipole distribution function by the field to follow in-phase with reversals of the field. With increasing frequency of alternations of the field the perturbation of the molecular dipole distribution function

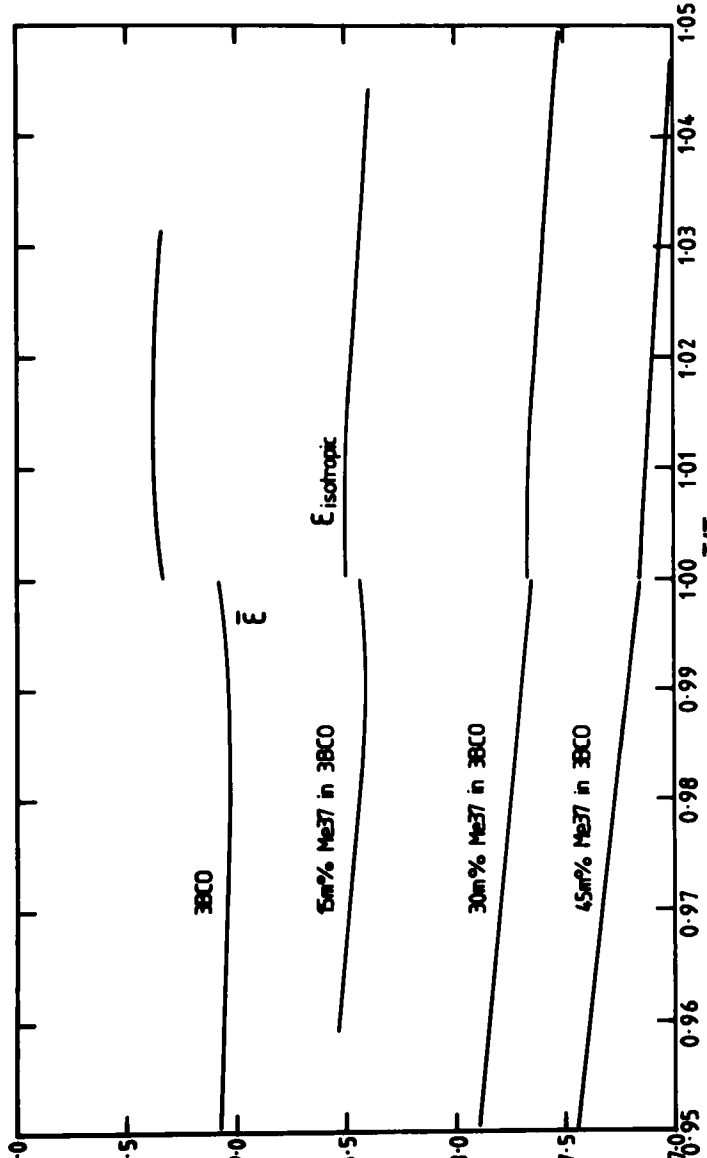

FIGURE 3 Mean permittivity of 3BCO/Me37 mixtures.[13]

TABLE V

Influence of molecular and fluid structure on the dielectric properties of a nematic fluid

Property	Influence of: molecular structure	fluid structure
μ	strong	slight if any
$\beta = \tan^{-1}(\mu_t/\mu_l)$	strong	may be significant
ϵ	strong	may be strong

will increasingly fail to follow the applied field, leading to a decrease in the corresponding component of the permittivity and the phenomenon of dielectric loss. In an anisotropic material such as a liquid crystal, one or more such losses may be seen at different frequencies in the parallel and perpendicular components of ϵ. The phenomenon is described quantitatively by generalizing the permittivity tensor to become a tensor function of frequency $\omega/2\pi$ with both real and imaginary parts:

$$\epsilon(\omega) = \epsilon'(\omega) - i\epsilon''(\omega) \tag{3.9}$$

The prototypic form for the frequency dependence due to a relaxation with frequency f_R is the Debye form:

$$\epsilon' = \epsilon_\infty + (\epsilon_s - \epsilon_\infty)/(1 + \omega^2\tau^2) \tag{3.10}$$

$$\epsilon'' = (\epsilon_s - \epsilon_\infty)\omega\tau/(1 + \omega^2\tau^2) \tag{3.11}$$

where

$$f_R = (2\pi\tau)^{-1} = \omega_R/2\pi \tag{3.12}$$

and all subscripts indicative of direction ($\parallel$ or $\perp$ to $\mathbf{n}$) have been omitted for simplicity. The significance of ϵ_s, ϵ_∞, and ω_R is clear from Figure 4 which shows both the real part ϵ' and the loss ϵ'' plotted against $\ln\omega$, together with a plot of the AC conductivity $\sigma = \omega\epsilon''$. An alternative presentation is the Cole-Cole plot in which ϵ'' is plotted against ϵ' with ω as a parameter (Figure 5). In this case Eqs. (3.10) and (3.11) give a semicircle centered on the x-axis. Experimental loss data is often fitted to the Fuoss-Kirkwood equation

$$\cosh^{-1}(\epsilon''_{max}/\epsilon'') = \alpha\ln|\omega\tau| \tag{3.13}$$

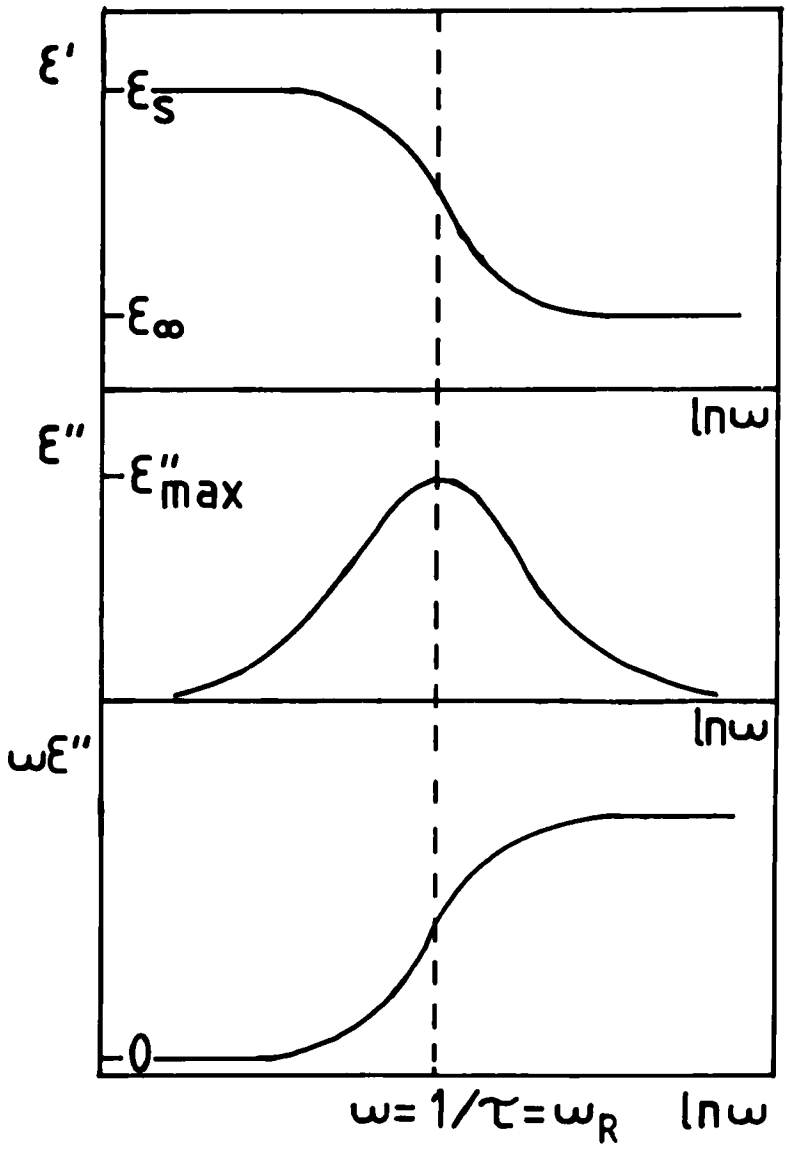

FIGURE 4 Representation of dielectric relaxation data as plots of real (ϵ') and imaginary (ϵ'') permittivity against frequency. Also shown is the plot of AC conductivity $\sigma = \omega\epsilon'$.

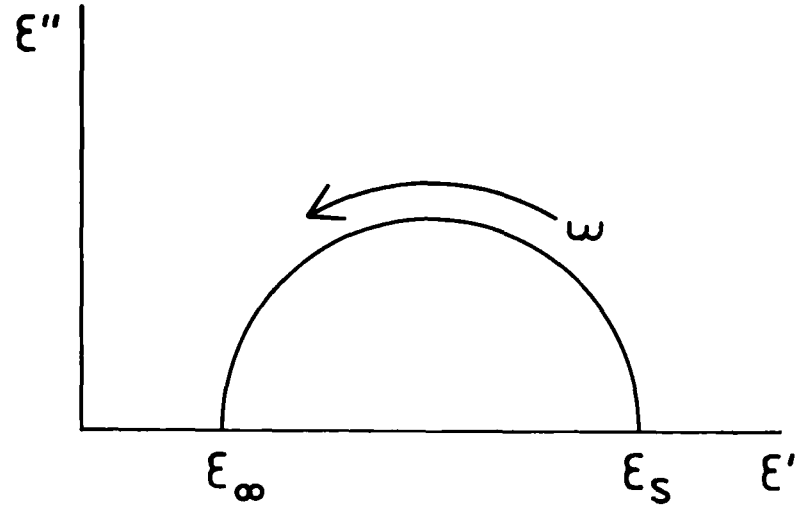

FIGURE 5 Representation of dielectric relaxation data as a Cole-Cole plot.

where the empirical parameter α normally lies between zero and unity, $\alpha = 1$ corresponding to the Debye form Eqs. (3.10), (3.11). Note that the decrement in the real part $\epsilon'_s - \epsilon'_\infty$ is given by

$$\epsilon'_s - \epsilon'_\infty = 2\epsilon''_{max}/\alpha \tag{3.14}$$

Since in general a molecule may have dipole components longitudinal and transverse to its "long axis," and with $S < 1$ each of these components may have non-zero projections both parallel and perpendicular to $\mathbf{n}$, one might predict four relaxations, two in each of $\epsilon_\parallel$ and $\epsilon_\perp$, with angular frequencies $\omega'_\parallel$, $\omega'_\perp$, $\omega'_\perp$, $\omega'_\parallel$.

Figure 6 shows the rotational diffusion modes involved in these relaxations. From Figure 6 one would predict that $\omega'_\parallel$ should be low because diffusion is hindered by the nematic pseudopotential, and that $\omega'_\perp \approx \omega'_\parallel$ since the same diffusional mode is involved. In agreement with this an anomalously low frequency relaxation in $\epsilon_\parallel$ together with a higher frequency relaxation at the same frequency in both $\epsilon_\parallel$ and $\epsilon_\perp$ are found experimentally in materials e.g. monoesters,[14] where the electric dipole clearly has both longitudinal and transverse components. Measurements of the magnitudes of the dielectric relaxations provides an interesting route to estimates of the order parameter S, the dipole moment μ, and the angle β between the molecular dipole and its "long axis."[14]

The very simple theoretical view implicit in Figure 6 is quantita-

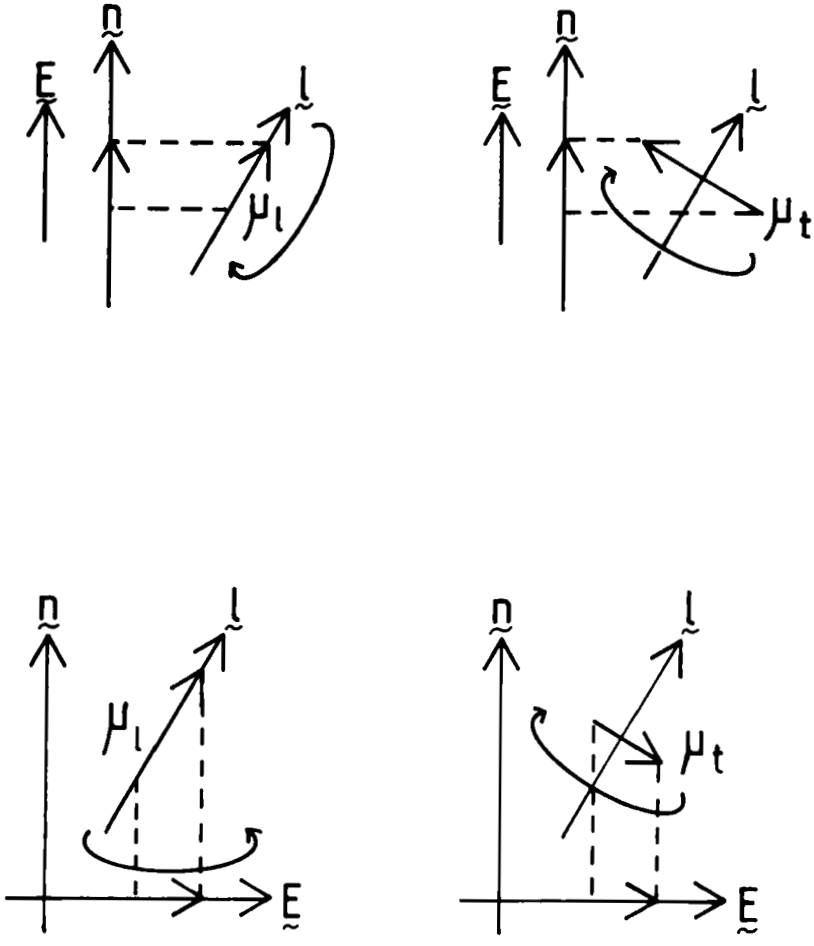

FIGURE 6 Rotational diffusion modes leading to dielectric relaxation in nematic liquids. The molecular "long axis" is denoted by **l**.

tively justifiable if the longitudinal component D_l^{rot} of the molecular rotational diffusion tensor is very much greater than its transverse component. More generally, a more rigorous diffusion model based on the work of Nordio *et al.*[15] appears acceptable. Application of such a model readily explains the experimental fact that the low frequency relaxation in $\epsilon_\parallel$ is invariably a good fit to the Debye form [Eqs. (3.10), (3.11)]. At first sight it is surprising to find a relaxation in an anisotropic liquid that is a much better fit to the Debye model than the relaxations in isotropic liquids which it was originally developed to describe!

3.4. Dual frequency materials

In some materials the lowest frequency relaxation in $\epsilon'_{\parallel}$ may be arranged so as to cause a reversal in the sign of $\Delta\epsilon$ at audio frequencies. A range of possible device applications based on "dual frequency addressing" with frequencies above and below the cross-over frequency f_0 (at which $\Delta\epsilon$ changes sign) may be envisaged.[16] Figure 7 defines the relevant dielectric parameters of such a dual-frequency material. Whereas the cross-over frequency f_0 is of device significance, the relaxation frequency f_R is of greater molecular significance. Since this relaxation obeys the Debye form,

$$f_0 = (\Delta\epsilon_L/|\Delta\epsilon_H|)^{1/2} f_R \tag{3.15}$$

The problems faced in the molecular engineering of f_R may be brought into focus by use of the rather simple approach of Maier and Saupe,[17] who write

$$f_R = f_D/g \tag{3.16}$$

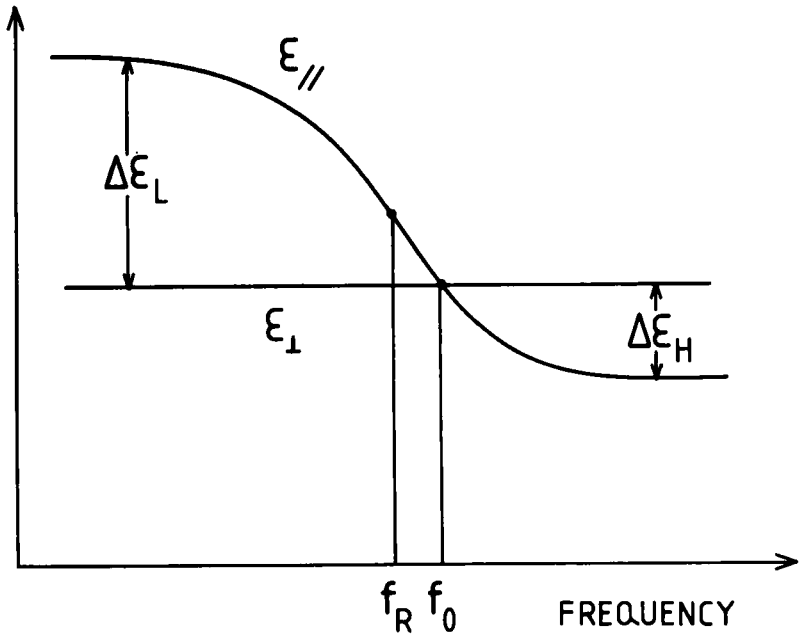

FIGURE 7 Definitions of dielectric parameters of a dual frequency material.

where f_D is a Debye-like relaxation frequency

$$f_D \propto \exp(-B/k_BT) \tag{3.17}$$

and

$$g \approx (k_BT/q)\exp(q/k_BT) \tag{3.18}$$

with

$$q = AST_c \tag{3.19}$$

where S is the order parameter and T_c the absolute clearing temperature. Thus

$$f_R \approx [CST_c/T]\exp[-(AST_c + B)/k_BT] \tag{3.20}$$

i.e. f_R has the form

$$f_R = f_D(T)/g(T/T_c) \tag{3.21}$$

a form which appears to be justifiable even in the more sophisticated diffusion-model approach of Nordio *et al.* A clear consequence of Eq. (3.21) is that neither constant absolute temperature T nor constant reduced temperature T/T_c is on its own a basis for comparison of the relaxation frequencies of different compounds.

The behaviour of the low frequency relaxation in mixtures is of both practical and theoretical interest. Mixtures of chemically similar compounds show a single relaxation and can apparently be regarded as a single-pseudocomponent fluid. Mixtures of chemically different components show distinct low frequency relaxations associated with each type of component. This has been demonstrated for mixtures of diesters with monoesters,[18] diesters with azoxy compounds,[19] and cyanoterphenyls with cyanobiphenyls.[20] In each case the mixtures show two distinct relaxations, clearly identifiable with the two types of compound present in the mixture (Figure 8). This observation forms the basis of a method for engineering practical mixtures for dual-frequency addressing.[14,21] One component (which may itself be a mixture) provides the low frequency relaxation, while the other (which has its lowest $\epsilon_\parallel$ relaxation at higher frequencies) is used to modify other macroscopic properties, particularly the viscosity, to desirable values. Since the practical applications call for both large

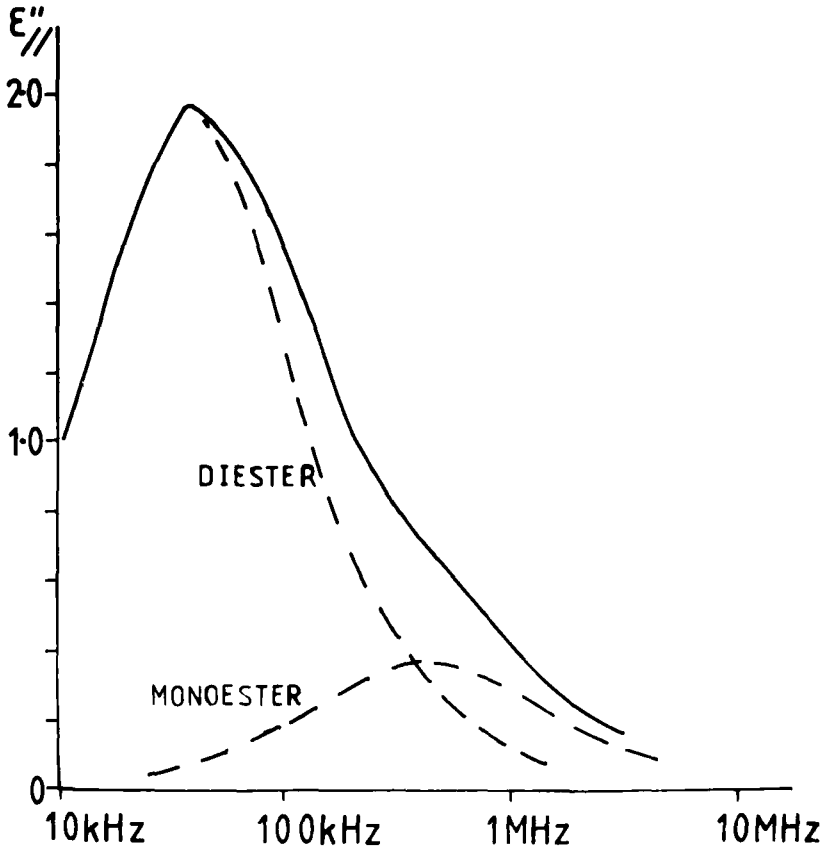

FIGURE 8 Mixtures of chemically dissimilar components show distinct low frequency relaxations associated with each type of component. The figure shows loss curves, $\epsilon''(\omega)$, for the lowest frequency relaxation in $\epsilon_{\parallel}$ of a diester/monoester mixture.[14,57]

$\Delta\epsilon_L$ and even larger $|\Delta\epsilon_H|$, there is a need for better negative $\Delta\epsilon$, low viscosity, materials for use in this second component.

Note, finally, that an obvious corollary of these observations is that the relaxation frequency does not usually correlate well with viscosity in mixtures.

4. SOME POINTS OF DIFFICULTY

In the previous sections we have discussed the macroscopic properties of liquid crystals making use of the simplest applicable theoretical concepts. Before proceeding further, it seems appropriate to draw

attention to some points of difficulty embedded within these (and indeed more sophisticated) concepts; points which are by no means fully resolved.

4.1. Internal field effects

As stated in Sec. 2, a property tensor measures the response of the system to an external field. If the tensor is to be defined as an intensive material property (and therefore independent of the size and shape of the sample) the field must be the local internal field at the point in the material being considered. This will not in general be equal to the "vacuum field" set up by the external sources of the field, since it will also contain contributions generated by the response of other parts of the material to the applied field.

Since $\epsilon \gg 1$ for condensed matter the permittivity is a prototypic example of this effect. Traditionally these corrections, associated with the names of Lorentz and others, have been calculated by considering small cavities cut into the continuum of material.[22] This procedure, unsatisfying even for isotropic materials, becomes even less desirable in an anisotropic fluid. In recent years the work of several authors has yielded a more satisfying approach, which has been applied to nematics by Madden and co-workers.[23,24] Here we outline briefly, and rather formally, only the most salient features.

The polarization in the material can be written in either of two ways:

$$\mathbf{P} = \epsilon_0 \boldsymbol{\chi} * \mathbf{E} = \epsilon_0 \boldsymbol{\chi}^0 * \mathbf{E}^0 \tag{4.1}$$

where

$$\boldsymbol{\chi} = \boldsymbol{\epsilon} - \mathbf{I} \tag{4.2}$$

is an intensive material property, but since $\mathbf{E}$, the internal field, depends on the thermodynamic state of the sample, $\boldsymbol{\chi}$ is not directly calculable from linear response theory. However, since $\mathbf{E}^0$, the vacuum field, is a true perturbation, $\boldsymbol{\chi}^0$ is directly calculable from linear response theory. The symbol $*$ is used in Eq. (4.1) to denote convolution type integrals; the equations become simple multiplications if Fourier transformed with respect to time and space. The relationship between $\mathbf{E}$ and $\mathbf{E}^0$ is

$$\mathbf{E}(\mathbf{r}, t) = \mathbf{E}^0(\mathbf{r}, t) + \int d^3\mathbf{r}' \mathbf{T}(\mathbf{r} - \mathbf{r}') \cdot \mathbf{P}(\mathbf{r}', t) \tag{4.3}$$

where the second-rank tensor

$$\mathbf{T}(\mathbf{r} - \mathbf{r}') = (4\pi\epsilon_0)^{-1}[3(\mathbf{r} - \mathbf{r}')(\mathbf{r} - \mathbf{r}')/|\mathbf{r} - \mathbf{r}'|^5 - \mathbf{I}/|\mathbf{r} - \mathbf{r}'|^3] \quad (4.4)$$

gives the field at $\mathbf{r}$ due to the polarization $\mathbf{P}(\mathbf{r}', t)$ at $\mathbf{r}'$. Hence Eqs. (4.3), (4.4) and (4.1) give the desired quantity χ in terms of the quantity χ^0 which can be calculated from linear response theory. This approach provides a more satisfying theory of internal field effects in the case of the permittivity tensor, and establishes a strategy which appears applicable to other internal field problems.

4.2. Definition of the "long axis"

Embedded in all of our discussion of the molecular origin of macroscopic properties, and indeed in more sophisticated treatments, is the concept of a preferred molecular frame. In the case of the "static" permittivity tensor the existence of both positive and negative $\Delta\epsilon$ shows clearly that the molecular electric dipole need not be parallel to this "long axis." Similarly the optical order parameter [Eq. (1.7)] may be written in molecular terms, taking $D = 0$, as

$$S_{op} = \tfrac{1}{2}(3\cos^2\beta - 1)S \quad (4.5)$$

where β is now the angle between the transition moment and the long axis. Since one may measure distinct S_{op} for distinct absorption transitions with moments that are known to be non-parallel,[3] one is again obliged to introduce a preferred molecular frame, to which each of the transition moments is referred with its value of β.

The question of whether the same preferred molecular frame is applicable to all macroscopic properties is one of great importance. If it is, then a unique set of molecular order parameters S, D, . . . (Sec. 1.2) is applicable to all macroscopic properties. Conversely, if a unique preferred molecular frame cannot be defined than neither are the order parameters unique.[25] The question therefore has an experimental test: do different macroscopic properties yield the same values for the molecular order parameters? Unfortunately, the estimation of molecular order parameters from measured macroscopic properties is not straightforward, and most if not all of the values in the literature are liable to errors and uncertainties of magnitude similar to the differences one might be seeking. However Tough and

Bradshaw[26] have shown that when well-conditioned estimation procedures are used, order parameters from refractive index and magnetic susceptibility measurements are in good agreement.

Any preferred frame of the molecule is a property of the fluid, not the molecule alone, and must therefore be determined experimentally. One natural candidate, appropriate to the macroscopic properties and measurement timescales of interest in device physics, is the principal axis frame of the rotational diffusion tensor.[14] The "long axis" is then the axis about which rotational diffusion is most rapid. This leads to the physically correct (but semantically unsatisfactory) conclusion that the "long axis" in a discotic nematic is perpendicular to the plane of the disc.[27]

4.3. Director fluctuations

The thermal fluctuations of the molecular orientation in nematics are of two kinds. The first are rapid, short wavelength, essentially one-molecule, fluctuations. Thermal averaging of these leads to the molecular orientational distribution function $f(\theta, \psi)$ introduced in Sec. 1.2. The second are slow, long wavelength, cooperative many-molecule fluctuations. They may be pictured as fluctuations in the principal axes of $f(\theta, \psi)$. They lead to characteristic light scattering by nematics. The separation of the thermal fluctuations into one-molecule and cooperative types is loosely analogous to the separation of electronic excitations into one-electron and plasmon modes in solids. In the case of molecular fluctuations in nematics it is not rigorously proven that the separation can be clearly and unambiguously made, but it is generally supposed that this is so, and that the cooperative fluctuations can therefore be treated as thermal fluctuations of the director $\mathbf{n}$ and thus are calculable from continuum nematodynamics (see Sec. 5).

Experimental measurements of macroscopic properties average, to a greater or lesser degree, over both types of fluctuation. A theoretical framework for describing this may be conveniently illustrated by taking as an example the permittivity tensor. We write [cf. Eq. (2.4)]

$$\epsilon_{ij}(\omega; \mathbf{r}, t) = \epsilon_{\perp}(\omega)\delta_{ij} + [\epsilon_{\parallel}(\omega) - \epsilon_{\perp}(\omega)]n_i(\mathbf{r}, t)n_j(\mathbf{r}, t) \quad (4.6)$$

where $\epsilon_{\parallel}(\omega)$, $\epsilon_{\perp}(\omega)$ are calculated using a clamped director and averaging over the one-molecule fluctuations only. The appearance of both ω and t as independent variables in Eq. (4.6) arises from the separation of fluctuation types discussed above. The value of ϵ_{ij} ob-

served in any experiment is obtained by appropriately averaging $\epsilon_{ij}(\omega; \mathbf{r}, t)$ over director fluctuations by use of continuum theory. In principle, therefore, the experimental value obtained for a macroscopic property depends on the spatial wavelengths $2\pi/k$ sampled by the measurement. These are different for different experiments, for example:

light scattering	$2\pi/k = \lambda(2\sin\frac{1}{2}\theta)^{-1} \sim 1$ to 10 μm
Freedericksz transition	$2\pi/k \leqslant 2d \sim 10$ to 100 μm

However, it is not obvious that this effect could ever be quantitatively large.

A second point, obvious from Eq. (4.6), is that director fluctuations couple $\parallel$ and $\perp$ components of the clamped-director tensor. For example, taking the z-axis as the average direction of the director:

$$\langle \epsilon_{zz}(\omega; \mathbf{r}, t)\rangle = \epsilon_{\perp}(\omega) + [\epsilon_{\parallel}(\omega) - \epsilon_{\perp}(\omega)]\langle n_z(\mathbf{r}, t)n_z(\mathbf{r}, t)\rangle \quad (4.7)$$

$$= \epsilon_{\parallel}(\omega)(1 - \delta) + \epsilon_{\perp}(\omega)\delta \quad (4.8)$$

where

$$1 - \delta = \langle n_z(\mathbf{r}, t)n_z(\mathbf{r}, t)\rangle < 1 \quad (4.9)$$

because of director fluctuations. This effect must clearly be borne in mind during the interpretation of data on macroscopic properties.[28] The extent to which different theories purporting to calculate macroscopic properties take into account director fluctuations is also a matter for debate.[29]

5. PARAMETERS OF CONTINUUM NEMATODYNAMICS

In previous sections we have discussed property tensors, taking as an example the permittivity tensor. Another classical category of macroscopic property is that of the coupling coefficients describing reactive or dissipative processes. The anisotropy of nematic fluids leads to much richer structure in these properties than for an isotropic fluid.

5.1. Notation

The additional complexity of the continuum mechanics of anisotropic media makes an efficient tensor notation essential. The notation widely used in continuum mechanics for Cartesian tensors is a little different to those used in some other fields:

vector **a** has components	a_i
derivatives	$\partial a_i/\partial x_j$, $\partial^2 a_i/\partial x_j \partial x_k$, etc
are written	$a_{i,j}$, $a_{i,jk}$, etc
2nd rank tensor **B** has components	B_{ij}
derivatives	$B_{ij,k}$, $B_{ij,kl}$, etc

and so on.

5.2. Curvature elasticity

We consider first the statics of a nematic liquid. As is well known, if F_d is the elastic free energy associated with distortion of $\mathbf{n}(\mathbf{r})$ from the state of uniform alignment $\mathbf{n}(\mathbf{r}) = \mathbf{n}_0$

$$F_d = \int \mathrm{d}^3\mathbf{r} f_d \tag{5.1}$$

where the free energy density f_d is given by

$$f_d = \tfrac{1}{2}\{K_{11}(n_{k,k})^2 + K_{22}(\epsilon_{ijk} n_i n_{k,j})^2 + K_{33}(n_{i,j} n_{i,k} n_j n_k) + K_{24}(n_{i,j} n_{j,i} - n_{i,i} n_{j,j})\} \tag{5.2}$$

$$= \tfrac{1}{2}\{K_{11}(\mathrm{div}\mathbf{n})^2 + K_{22}(\mathbf{n} \cdot \mathrm{curl}\mathbf{n})^2 + K_{33}(\mathbf{n} \times \mathrm{curl}\mathbf{n})^2 + K_{24}\mathrm{div}[(\mathbf{n} \cdot \mathrm{grad})\mathbf{n} - \mathbf{n}\mathrm{div}\mathbf{n}]\} \tag{5.3}$$

where K_{11}, K_{22}, and K_{33} are respectively the splay, twist, and bend elastic constants (a fact remembered by the mnemonic STaB), and the convention of summation over repeated indices is assumed. By the divergence theorem the term containing K_{24} contributes only to surface energies and is therefore not needed in the case of disclination-free material with strong-anchoring boundary conditions.

5.3. Extension to smectic A phase

If it is assumed that when a smectic A is distorted the number of "layers" lying between two points A and B is constant, then

$$t_s^{-1} \int_A^B \mathbf{n} \cdot \mathrm{d}\mathbf{l} = \text{constant} \tag{5.4}$$

where t_s is the wavelength of the mass density wave (Sec. 1.3). Hence if the integral is taken round a closed curve C bounding a surface S

$$0 = t_s^{-1} \int_C \mathbf{n} \cdot \mathrm{d}\mathbf{l} = t_s^{-1} \int_S \mathrm{curl}\mathbf{n} \cdot \mathrm{d}\mathbf{S} \tag{5.5}$$

implying that curl**n** must vanish and that K_{22} and K_{33} must diverge in the S_A phase. Hence

$$f_d = \tfrac{1}{2}K_{11}(\mathrm{div}\mathbf{n})^2 + \text{compressibility terms} \tag{5.6}$$

If we consider a "layer" with principal radii of curvature R_1 and R_2

$$\tfrac{1}{2}K_{11}(\mathrm{div}\mathbf{n})^2 = \tfrac{1}{2}K_{11}(R_1^{-1} + R_2^{-1})^2 \tag{5.7}$$

$$= 0 \text{ if } R_1 = R_2 = \infty \text{ or } R_1 = -R_2 \tag{5.8}$$

demonstrating that the term containing K_{11} vanishes both for flat "layers" and for saddle-shaped "layers" with equal but opposite radii of curvature.

This simple calculation[30] emphasizes the ease with which S_A phases can distort from uniform alignment with flat "layers" and constant **n**. The development of such distortions ("textures") on passing from an aligned nematic into the smectic phase may cause spurious changes in the apparent values of macroscopic properties.

5.4. Influence of the S_A phase on nematic elastic constants

The prediction that K_{22} and K_{33} diverge in the S_A phase would lead one to suppose that interesting behaviour might be seen in the nematic phase if a smectic phase was approached by changing temperature or composition. The elastic constants of nematics have been extensively studied with the aim of engineering low K_{33}/K_{11} desired for high multiplexability of TN LCDs. One of the more surprising results to emerge from such studies is that K_{11} may also diverge on approaching an S_A phase. This occurs, for example, on approaching the

"injected" S_A phase observed near the centre of the composition range in mixtures of 4-*n*-alkyl-4′-cyanobiphenyls and 4-*n*-alkylphenyl-4′-*n*-alkylbenzoates.[31] The S_A phase in such cases is of "monolayer" type i.e. the wavelength of the mass density wave is approximately equal to one molecular length. As the smectic A phase is approached by varying the composition, K_{11} diverges sooner but more weakly than K_{33}, causing K_{33}/K_{11} first to fall and then increase rapidly and diverge. At temperatures above that at which the smectic is encountered, its effect is still manifest as a lowering of K_{33}/K_{11}. Divergence of K_{11} does not appear to have been seen in the "bilayer" type of S_A where the mass density wavelength is approximately twice the molecular length (e.g. S_A phases of cyanobiphenyl materials alone).[32]

Grinstein and Pelcovits[33] have argued that anharmonic terms needed in the free energy expression for the S_A phase lead to weak divergence of K_{11}. On their argument any difference between "monolayer" and "bilayer" smectics is presumably quantitative rather than qualitative. Their argument is focussed on the smectic phase, and predicts behaviour in the nematic only by implication. We point out that the director fluctuations discussed in Sec. 4.3 imply that in the nematic phase

$$K_{11} = K_{11}^0(1 - \delta) + K_{33}^0\delta \tag{5.9}$$

where K_{11}^0, K_{33}^0 are calculated with the director clamped, and δ is the mixing coefficient arising from director fluctuations. It would be of interest to calculate δ as the smectic phase is approached. Since K_{33}^0 will diverge and δ must vanish, the term $K_{33}^0\delta$ might either diverge or vanish according to the relative rates at which K_{33}^0 and $1/\delta$ diverge, thus causing K_{11} either to diverge or not, even though K_{11}^0 did not diverge. Although superficially very different to the Grinstein-Pelcovits theory, such an approach might in reality be equivalent, due fundamentally to the connection between fluctuations and the change in symmetry on passing from the nematic to the S_A phase.

5.5. Electrohydrostatics of a "Laminar" LCD

The distortion of the director configuration in a thin liquid crystal film by application of an electric field is important not only because of its practical application in the TN LCD, but also because such Freedericksz-type transitions are of fundamental interest and the basis of methods for the measurement of macroscopic parameters such as

elastic constants. The simplest type of device, and one of great practical interest, is the "laminar" LCD in which the director tilt and twist angles α and β (Figure 9) are functions only of the coordinate z perpendicular to the plane of the cell.

$$\alpha = \alpha(z) \qquad \beta = \beta(z) \tag{5.10}$$

The application of Maxwell's equations to a laminar LCD in equilibrium is straightforward in the case when the liquid crystal is highly resistive and conductivity can be neglected.[34] Both div**D** and curl**E** vanish giving

$$D_z = \text{constant} \tag{5.11}$$

and

$$E_x = E_y = 0 \tag{5.12}$$

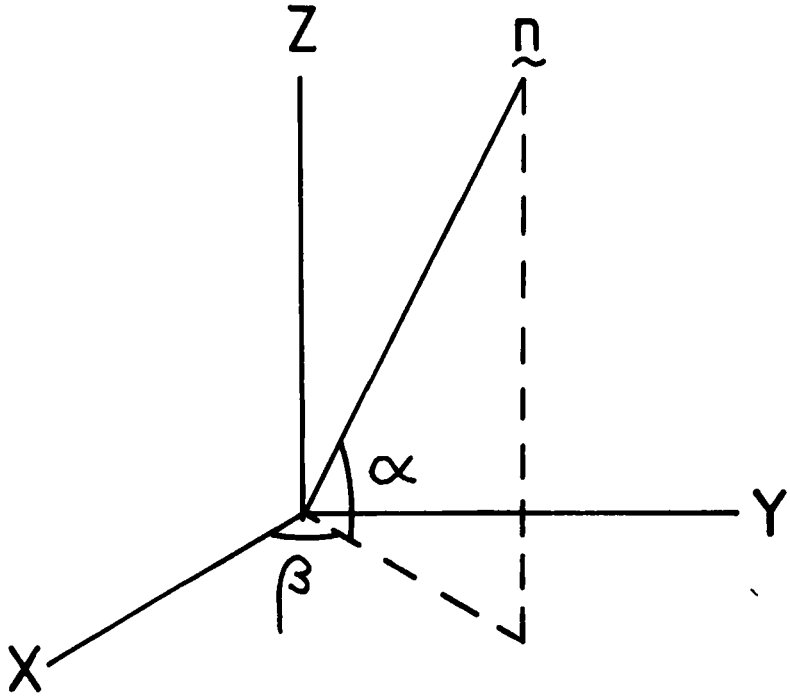

FIGURE 9 Definition of director tilt and twist angles α and β respectively.

respectively. If the voltage across the cell is V, then

$$V = \int_0^d E_z \, dz = (D_z/\epsilon_0)\int_0^d dz/\epsilon_{zz} \tag{5.13}$$

and its capacitance per unit area C is given by

$$1/C = \epsilon_0^{-1} \int_0^d dz/\epsilon_{zz} \tag{5.14}$$

where

$$\epsilon_{zz} = \epsilon_{\parallel} \sin^2\alpha + \epsilon_{\perp} \cos^2\alpha \tag{5.15}$$

Evaluation of the integrals in Eqs. (5.13) and (5.14) requires an expression for $d\alpha/dz$ from the detailed continuum statics of nematics.

Non-zero conductivity of the liquid crystal, whether due to carriers or dielectric loss, can be described by use of the complex permittivity tensor [Eq. (3.9)]. In general, it is essential to consider the Fourier transform (with respect to time) of the voltage applied to the cell. For the component with frequency $\omega/2\pi$, Eq. (5.11) becomes

$$i\omega D_z + j_z = \text{constant} \tag{5.16}$$

where j_z is the z component of the current density. It is convenient to define the integrals

$$\mathrm{I}' = \int_0^d dz \, \epsilon'_{zz}/(\epsilon'^2_{zz} + \epsilon''^2_{zz}) \tag{5.17}$$

$$\mathrm{I}'' = \int_0^d dz \, \epsilon''_{zz}/(\epsilon'^2_{zz} + \epsilon''^2_{zz}) \tag{5.18}$$

and the Q-factor

$$Q = \omega CR \tag{5.19}$$

The analogues of Eqs. (5.13) and (5.14) are then

$$V = (D_z\mathrm{I}' + \omega^{-1} j_z \mathrm{I}'')/\epsilon_0 \tag{5.20}$$

$$Q = I'/I'' \tag{5.21}$$

$$1/C = I'(1 + Q^{-2})/\epsilon_0 \tag{5.22}$$

$$R = I''(1 + Q^2)/\omega\epsilon_0 \tag{5.23}$$

The case of non-zero conductivity has not, in the past, been adequately treated in the literature. However, a correct account,[35] derived independently prior to this review, has appeared during the preparation of this written version.

The application of Maxwell's equations to a *non-equilibrium* laminar LCD would seem to merit investigation. Although present practice in treating problems where the director is moving (and hence the nematic is flowing) may be quantitatively adequate, we offer the following quotation both as evidence that a rigorous treatment is desirable and as reason for not attempting one here: "The problem of formulating constitutive equations for moving and deforming material media is one of the most difficult and controversial in electromagnetic theory."[36]

5.6. Nematodynamics

Given the inevitable complexity of the hydrodynamics of an anisotropic fluid with two hydrodynamic variables, $\mathbf{v}(\mathbf{r}, t)$ and $\mathbf{n}(\mathbf{r}, t)$, it is relevant to ask whether the dynamics of liquid crystals is a subject of unavoidable practical concern. The answer is yes, for a number of reasons:

(a) *Non-Newtonian "viscosity"*

In conventional viscometric experiments the apparent viscosity coefficient may depend on shear rate, geometry of the apparatus, etc. These effects do not arise from changes in the molecular order parameters (the kinetic energy per molecule associated with normal macroscopic flows is only a tiny fraction, 10^{-5} or less, of the intermolecular interaction energy per molecule). They arise from competition between the flow-induced orientation of $\mathbf{n}$ and that induced by the boundaries of the sample.

(b) *Turn-on and turn-off times of LCDs*

For example, the natural turn-off of a TN LCD is not even approximately a simple exponential decay.

(c) *Coupling of fluid flow and director reorientation*

In general it is not possible to have one without the other, and understanding of this coupling is therefore essential to an understanding of the device physics of LCDs.

(d) *(Electro)hydrodynamic instabilities*

The motion of the director may do something unexpectedly different, and perhaps advantageous or detrimental to device performance, above some threshold in the drive level.

The additional macroscopic parameters required to describe the dynamics of nematics may be presented in a number of forms, all of which may be related to the α coefficients appearing in the Leslie-Ericksen equations.[37] These equations introduce dynamical contributions to the stress tensor $\bar{t}_{ij}$ and to the intrinsic body force on the director $\bar{g}_i$, which are the most general allowed by symmetry subject to the constraints of linearity in fluid velocity and rate of director reorientation:

$$\bar{t}_{ij} = \alpha_1 n_k n_p A_{kp} n_i n_j + \alpha_2 N_i n_j + \alpha_3 N_j n_i + \alpha_4 A_{ij} + \alpha_5 A_{ik} n_k n_j + \alpha_6 A_{jk} n_k n_i \quad (5.24)$$

$$\bar{g}_i = -\gamma_1 N_i - \gamma_2 A_{ik} n_k \quad (5.25)$$

where

$$\gamma_1 = \alpha_3 - \alpha_2 \quad (5.26)$$

$$\gamma_2 = \alpha_6 - \alpha_5 \quad (5.27)$$

$$A_{ij} = \tfrac{1}{2}(v_{i,j} + v_{j,i}) \quad (5.28)$$

$$N_i = \dot{n}_i - \omega_{ik} n_k \quad (5.29)$$

$$\omega_{ik} = \tfrac{1}{2}(v_{i,k} - v_{k,i}) \quad (5.30)$$

and, as usual, repeated indices imply summation. On a point of semantics, note that although the theory is linear in the sense of being linear in shear rates it is highly non-linear in the sense of leading to non-linear equations of motion.

Of the six coupling coefficients $\alpha_1, \ldots, \alpha_6$ appearing in Eqs. (5.24)

and (5.25), only 5 are independent since the Onsager reciprocal relationships imply the Parodi relation[38]

$$\alpha_6 - \alpha_5 = \alpha_3 + \alpha_2 = \gamma_2 \tag{5.31}$$

The 5 independent quantities can be formulated as 4 dissipative coefficients and one reactive coefficient. The dissipative coefficients may be visualized by imagining the director to be clamped (e.g. by an infinite external field) relative to various flow patterns. Figure 10 shows the three configurations associated with the early work of Miesowicz[39] and corresponding to the linear combinations

$$\eta_1 = \tfrac{1}{2}(-\alpha_2 + \alpha_4 + \alpha_5) \tag{5.32}$$

$$\eta_2 = \tfrac{1}{2}(\alpha_3 + \alpha_4 + \alpha_6) \tag{5.33}$$

$$\eta_3 = \tfrac{1}{2}\alpha_4 \tag{5.34}$$

Note that other labellings of the Miesowicz η coefficients are also to be found in the literature, including different assignments of the subscripts 1, 2, 3. The fourth dissipative coefficient α_1, also written η_{12}, is perhaps most usefully visualized by considering the effective viscosity η_{eff} in the plane of shear (associated with $\bar{t}_{zx}$) for a director clamped in a direction (θ, ϕ) relative to uniform shear due to a velocity field $(0, 0, v_z(x))$ as shown in Figure 11:

$$\eta_{\text{eff}} = \eta_1 \sin^2\theta \cos^2\phi + \eta_2 \cos^2\theta + \eta_3 \sin^2\theta \sin^2\phi + \eta_{12} \cos^2\theta \sin^2\theta \cos^2\phi \tag{5.35}$$

From Eq. (5.35) it is evident that $\eta_{12}(=\alpha_1)$ vanishes from the expression for η_{eff} for the three Miesowicz configurations but not, in general, for intermediate configurations.

The fifth coefficient may be taken as

$$\lambda = -\gamma_2/\gamma_1 = (1 + \alpha_3/\alpha_2)/(1 - \alpha_3/\alpha_2) \tag{5.36}$$

and is reactive in character, describing the coupling between flow and director orientation.

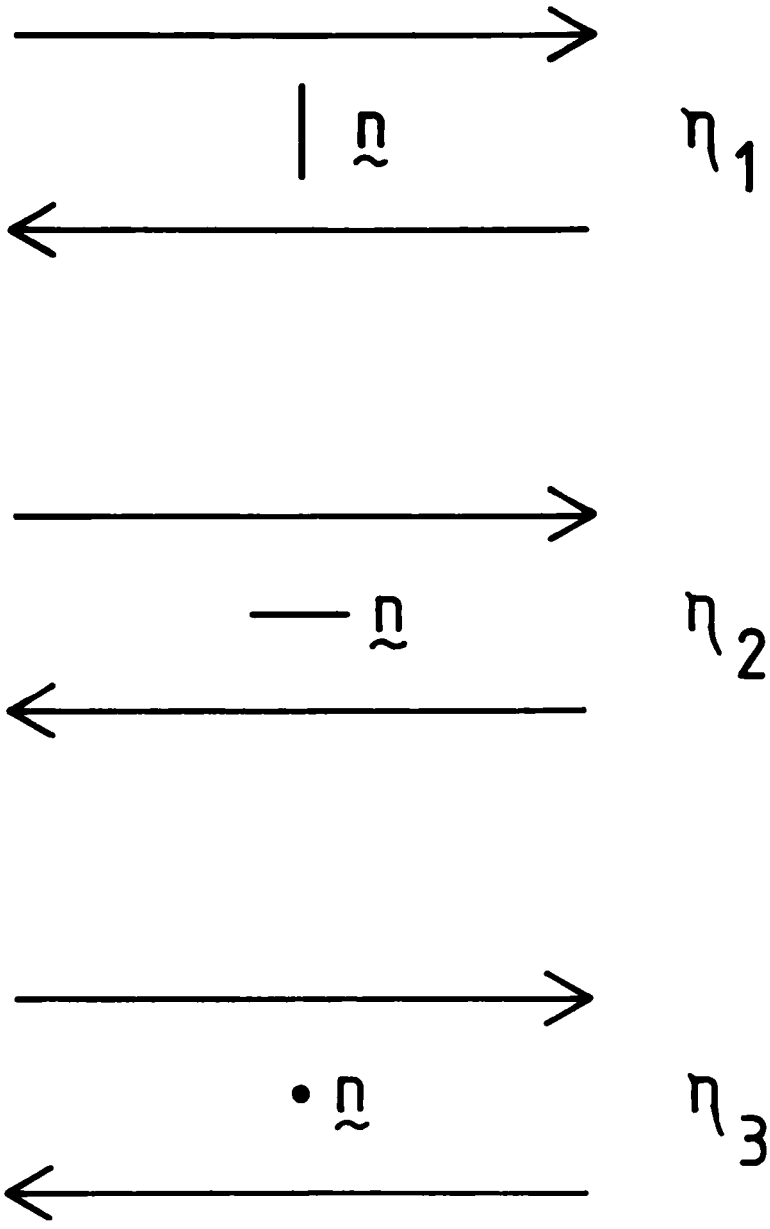

FIGURE 10 The three Miesowicz configurations; the diagrams show the relative orientations of the velocity shear and the clamped director **n**.

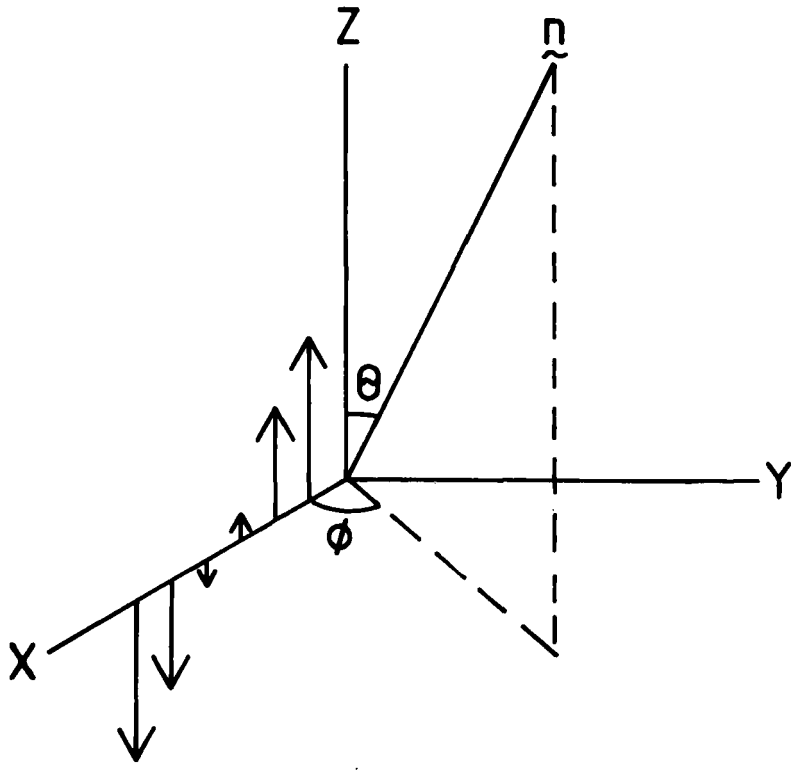

FIGURE 11 Uniform shear configuration considered in the text.

5.7. Solutions of the Leslie-Ericksen equations

It is helpful to consider briefly some basic points concerning the solutions of the Leslie-Ericksen equations.

(a) *Scaling*

The Leslie-Ericksen equations are invariant under the tranformation

$$\mathbf{r}' = c\mathbf{r} \qquad t' = c^2 t \tag{5.37}$$

where c is a scaling factor. This has been verified experimentally, and illustrates clearly the overdamped (diffusive) nature of nematodynamics.

(b) *Neglect of inertial term*

The analogy with diffusive motion is even stronger in a liquid crystal device since the term $\rho\dot{\mathbf{v}}$, where ρ is the density of the fluid, can usually be neglected. For an LCD with cell spacing d the time taken for $\mathbf{v}$ to adjust to a change in $\mathbf{n}$ is of order $\rho d^2/\eta$ which $\sim 10^{-6}$ s for $d \sim 10\ \mu$m, whereas the time scale characteristic of director motions is $\geqslant 10^{-3}$ s.

(c) *Special solutions in uniform shear*

Two special solutions, in which the director is stationary despite the presence of flow, are worthy of note. Referring to Figure 11, first, if $\phi = 0$ the viscous torque on the director is

$$\Gamma_{visc}(\phi = 0) = v_z'(\alpha_2 \sin^2\theta - \alpha_3 \cos^2\theta) \tag{5.38}$$

where $v_z' = dv_z/dx$ is the shear. From Eq. (5.28) this torque vanishes for a "flow alignment angle" θ_0 given by

$$\theta_0 = \tan^{-1}(\alpha_3/\alpha_2)^{1/2} \qquad \text{if} \qquad (\alpha_3/\alpha_2) > 0 \tag{5.39}$$

The sign of θ_0 is such that $\lambda n_x n_z v_z' > 0$. When $(\alpha_3/\alpha_2) < 0$ the flow alignment angle θ_0 is imaginary. Second, if $\theta = \pi/2$, $\phi = \pi/2$ i.e. $\mathbf{n} = (0, 1, 0)$ the viscous torque again vanishes, although this solution is unstable above some finite shear.

(d) *Numerical solution*

Since for a parallel aligned cell the Leslie-Ericksen equations yield two coupled partial differential equations, while for a twisted cell they yield four, their solution by numerical techniques is an attractive approach to obtaining reasonable generality, which has been advanced particularly by the work of Berreman.[40] An early success of this approach was the demonstration of how the coupling of flow to director orientation led to fluid "backflow" and director "kickback" effects.[41]

5.8. Measurement of viscous coefficients

Space does not permit even a cursory survey of the various methods which have been proposed for measuring the viscous coefficients. Much interesting experimental work has been done in this area, and

various of the viscous coefficients have now been determined for a number of nematic materials. However, in the opinion of the present author at least, none of the methods fully satisfies the criteria set out in Table I. Light scattering, perhaps the most attractive on grounds of sample size and computer control, has a problem that an applied electric field (needed if coefficients other than γ_1 are to be extracted with high accuracy) leads to unexpected effects in the splay-bend mode, thus involving additional macroscopic parameters.[42] It is also demanding with respect to sample preparation, since stray light scattered by e.g., alignment defects, must be avoided. Shear wave reflectance is also economical with respect to sample size, but measures only α_4 and the rather awkward combination

$$\eta_B = \tfrac{1}{2}[\alpha_4 + \alpha_6 - (\alpha_3\gamma_2/\gamma_1)] \tag{5.40}$$

The third combination which appears in the theory

$$\eta_C = \tfrac{1}{2}[\alpha_4 + \alpha_5 - (\alpha_2\gamma_2/\gamma_1)] \tag{5.41}$$

is equal to η_B even without recourse to the Parodi relation Eq. (5.31). The technique is experimentally demanding with respect to temperature control.

The various viscometric methods which have been developed depend on measuring the effective viscosity with the director "clamped" with an external field. From Eq. (5.35) four independent configurations are required to get η_1, η_2, η_3, and η_{12}. If $\alpha_3/\alpha_2 > 0$ measurement of θ_0 completes the set of coefficients. Both these and the related experiments of torsional shear flow (Wahl and Fischer[43]) and torque induced by a rotating magnetic field (Zvetkow[44]) suffer in varying degrees from some or all of the problems that:

(i) the theory usually used assumes an ideal situation not fully satisfied in practice, e.g., aligning field not infinite, wall and/or edge effects non-negligible, etc;

(ii) the behaviour of materials with $\alpha_3/\alpha_2 < 0$ is not fully understood;

(iii) a large sample is required.

In addition the two last-mentioned experiments measure only, for the torsional shear flow, α_2 and α_3 (at best) and, for the rotating magnetic field, γ_1.

Of the various viscous coefficients γ_1 is probably the most accessible, being relatively easily measured by either a Zvetkow-type experiment or by light scattering.

6. SOME ISSUES IN THE PHENOMENOLOGY OF NEMATIC VISCOSITY

6.1. Temperature and order parameter dependence of viscous coefficients

It is generally supposed on both theoretical and empirical grounds that the temperature dependence of the viscous coefficients is likely to be of the form

$$\eta \sim A(S)\exp[E(S)/k_BT] \tag{6.1}$$

However, the order parameter dependence of the coefficients A and E introduces a weak temperature dependence which is difficult to verify experimentally against the background of the strong exp[const./T] dependence, particularly since the experimentally-accessible range of S is usually small. Little, if any, thought has been given to the implications of $D \neq 0$ for the theoretical forms of the viscous coefficients.

6.2 Flow alignment—and lack of it

The question of whether, and at what temperatures, a nematic material has imaginary flow alignment angle θ_0 is of practical importance both because some theories of experiments to measure viscous coefficients assume θ_0 is real, and because θ_0 being imaginary may introduce new hydrodynamic instabilities into device behaviour.

To the best of our knowledge all nematics having smectic A phases show imaginary θ_0 over part or all of their nematic range, together with some materials not showing a smectic phase.[45,46] The existence of imaginary θ_0 has no obvious correlation with molecular polarity or the presence specifically of "bilayer" smectic-like local order due to a terminal CN substituent,[45] although the presence of some kind of smectic-like local order is presumably always the source of the phenomenon, even in those materials not showing a detectable smectic phase. All dual-frequency materials (Sec. 3.4) known to the author show imaginary θ_0 over at least part of their nematic range[47] (although imaginary θ_0 is not, of course, a sufficient condition for dual-frequency behaviour).

6.3. Divergencies at S_A phase

If we imagine smectic A "layers" forming perpendicular to the director in Figure 11, these "layers" will be disrupted by the flow unless

$\theta = \pi/2$. From inspection of Eq. (5.35), this suggests that at least η_2, and possibly η_{12}, may diverge on approaching an S_A phase. A similar argument applied to an irrotational flow verifies that η_{12} should also diverge. Translated into α coefficients, the conclusion, confirmed both by more rigorous theory[48] and by experiment,[45,49] is that α_1, α_3, and α_6 [cf. Eq. (5.31)] diverge on approaching a smectic A phase. As with the elastic constants (Sec. 5.4), the influence of divergencies at the smectic phase is felt over a significant proportion of the nematic range, and knowledge of such divergencies can therefore be used to engineer the viscous properties of the nematic phase.

There is some evidence that, as with the divergence of K_{11} discussed in Sec. 5.4, the divergence of α_3, at least, is weaker in some S_A phases than others. Evidence of weak divergence in "bilayer"-type cyanobiphenyl materials and strong divergence in non-cyano materials has come from shear cell studies,[45] and from NMR estimates[50] of γ_1.

6.4. "Bulk" viscosity

It is universal practice in the LC materials industry to characterise the viscosity of their products by a single number obtained by measuring in a conventional viscometer and treating the data as if the liquid were isotropic. There is no doubt that the result is a useful empirical number which correlates at least approximately with the response times of twisted nematic and other types of LC device. It is equally obvious that the number is ill-defined and its meaning is unclear. Somewhat surprisingly, the industry does not usually take into account that this bulk viscosity may be strongly dependent on shear rate or geometry (although such effects would be expected and, indeed, can be verified experimentally).[51] Equally, published data[52] shows no qualitative distinction between materials with real θ_0 and those with imaginary θ_0. Both of these points suggest that the numbers usually reported may not be "flow aligned" viscosities, contrary to what has sometimes been stated or implied in the literature.

To the extent that the published "bulk viscosity" really is as well-behaved a parameter as has been found or assumed, the work of Cladis and coworkers[53] may be significant. These authors suggest that in some typical viscometric situations the liquid may in fact contain large numbers of disclinations. The hydrodynamics of a nematic containing a continuous density of disclinations may be worked out by use of gauge theory.[54] A rough guide to the shear rates at which disclinations might begin to form is given by the (dimensionless) Ericksen number

$$\mathrm{Er} = \eta d^2 v'/K \tag{6.2}$$

where d is the thickness of the sheared sample, v' is the shear rate, and η and K are appropriate viscous and elastic coefficients. The literature on hydrodynamic instabilities would suggest that in constant shear disclinations begin to form when Er exceeds a number of order 10. (In oscillatory shear the critical Er apparently increases with frequency; for example, a linear increase with frequency was found in shear cell studies at audio frequencies.)[45] Clearly there is a need for the experiments used to measure bulk viscosity to be performed with apparatus in which shear rate and surface alignment can be controlled and, equally important, the sample can be observed visually during shear.

The temperature dependence of the bulk viscosity can be fitted to the Vogel-Fulcher law

$$\eta = \eta_0 \exp[b/(T - T_0)] \tag{6.3}$$

where T_0 is a temperature close to the glass transition temperature. This form of temperature dependence is associated with glass formation and, perhaps more significantly in the present context, with free volume effects.[55,56] Clearly the fact that bulk viscosity data can be fitted to Eq. (6.3) raises questions concerning the temperature dependencies of the viscous coefficients; questions which are difficult to answer while the way in which individual α coefficients contribute to η_{bulk} remains unknown and experimental data on the α coefficients is limited.

7. CONCLUDING REMARKS

In conclusion it may be helpful to summarise the following salient points:

(i) Both continuum and molecular views of macroscopic properties have unresolved points of difficulty even for nematics.

(ii) Molecular engineering of LCs is about optimising both molecular *and* fluid structure.

(iii) There is a continuing need for calculations relating device behaviour to macroscopic properties.

(iv) There is a continuing need for improved measurement techniques and more data.

Finally, in this age of information technology, we offer one further point for discussion: is there a need for an international computerized data base of LC macroscopic properties?

Acknowledgments

I am grateful to my colleagues in RSRE and elsewhere for the many collaborations and discussions which have contributed directly or indirectly to this review; and especially I thank Dr. M. J. Bradshaw and Dr. P. A. Madden for helpful discussions.

References

1. D. M. Brink and G. R. Satchler, *Angular Momentum*, 2nd Ed. (Clarendon Press, Oxford, 1968).
2. G. R. Luckhurst, in *The Molecular Physics of Liquid Crystals*, eds. G. R. Luckhurst and G. W. Gray (Academic Press, London, 1979), Chap. 4.
3. M. G. Clark and F. C. Saunders, *Mol. Cryst. Liq. Cryst.*, **82**, 267 (1982).
4. G. R. Luckhurst, *10th Internat. Liq. Cryst. Conf.* (York, UK, 1984), Paper A52.
5. R. Y. Dong and E. T. Samulski, *Mol. Cryst. Liq. Cryst.*, **82**, 73 (1982).
6. A. J. Leadbetter, in *The Molecular Physics of Liquid Crystals*, eds. G. R. Luckhurst and G. W. Gray (Academic Press, London, 1979), Chap. 13.
7. W. Maier and G. Meier, *Z. Naturforsch.*, **16a**, 262 (1961).
8. L. M. Blinov, *Electo-Optical and Magneto-Optical Properties of Liquid Crystals* (J. Wiley, Chichester, 1983), Sec. 2.4.1.
9. Table III is based on data collected by M. J. Bradshaw in her Ph.D. thesis (University of Exeter, 1984), together with additional dipole moment data provided by E. P. Raynes (personal communication).
10. T. Inukai, K. Furukawa and H. Inoue, *8th Internat. Liq. Cryst. Conf.* (Kyoto, Japan, 1980), Paper E-11P.
11. M. Schadt, *Mol. Cryst. Liq. Cryst.*, **89**, 77 (1982).
12. R. Eidenschink, G. Haas, M. Römer and B. S. Scheuble, *Angew. Chem. Internat. Ed. Engl.*, **23**, 147 (1984).
13. M. J. Bradshaw and E. P. Raynes, *Mol. Cryst. Liq. Cryst.*, **91**, 145 (1983).
14. M. F. Bone, A. H. Price, M. G. Clark and D. G. McDonnell, *Liq. Cryst. Ordered Fluids*, **4**, 799 (1984).
15. P. L. Nordio, G. Rigatti and U. Segre, *Mol. Phys.*, **25**, 129 (1973).
16. H. K. Bücher, R. T. Klingbiel and J. P. Van Meter, *Appl. Phys. Lett.*, **25**, 186 (1974); M. G. Clark, *Microelectron. Reliab.*, **21**, 887 (1981).
17. G. Meier and A. Saupe, *Mol. Cryst.*, **1**, 515 (1966).
18. L. Bata and G. Molnár, *Chem. Phys. Lett.*, **33**, 535 (1975).
19. M. I. Barnik, L. M. Blinov, A. V. Ivashchenko and N. M. Shtykov, *Sov. Phys. Crystallogr.*, **24**, 463 (1979).
20. H. R. Zeller, *Phys. Rev. A*, **23**, 1434 (1981).
21. D. G. McDonnell and R. A. Smith, *9th Internat. Liq. Cryst. Conf.* (Bangalore, India, 1982), Paper J-10.
22. C. J. F. Böttcher and P. Bordewijk, *Theory of Electric Polarization*, 2nd Ed. (Elsevier, Amsterdam), Vol. I (1973), Vol. II (1978).
23. P. A. Madden and D. Kivelson, *Advan. Chem. Phys.*, **56**, 467 (1984).
24. D. M. F. Edwards and P. A. Madden, *Mol. Phys.*, **48**, 471 (1983).

25. F. C. Frank, *Proc. Internat. Conf. Liq. Cryst. Bangalore 1979*, ed. S. Chandrasekhar (Heyden, London, 1980), p. 1, and *Phil. Trans. Roy. Soc. (Lond.)*, **A309**, 71 (1983).
26. R. J. A. Tough and M. J. Bradshaw, *J. Phys. (Paris)*, **44**, 447 (1983).
27. M. G. Clark, *Phil. Trans. Roy. Soc. (Lond.)*, **A309**, 74 (1983).
28. P. A. Madden, unpublished work.
29. M. Warner, *Mol. Phys.*, **52**, 677 (1984).
30. T. E. Faber and G. R. Luckhurst, *Ann. Rept. Progr. Chem.*, **72A**, 31 (1975).
31. M. J. Bradshaw and E. P. Raynes, *Mol. Cryst. Liq. Cryst.*, **99**, 107 (1983).
32. N. V. Madhusudana and R. Pratibha, *Mol. Cryst. Liq. Cryst.*, **89**, 249 (1982).
33. G. Grinstein and R. A. Pelcovits, *Phys. Rev. Lett.*, **47**, 856 (1981); T. C. Lubensky, G. Grinstein and R. A. Pelcovits, *Phys. Rev. B*, **25**, 6022 (1982).
34. H. J. Deuling, *Mol. Cryst. Liq. Cryst.*, **19**, 123 (1972).
35. R. N. Thurston, *Mol. Cryst. Liq. Cryst.*, **108**, 61 (1984).
36. C. Truesdell and R. Toupin, *The Classical Field Theories, Handb. Phys.*, **III/1**, 226 (1960).
37. F. M. Leslie, *Advan. Liq. Cryst.*, **4**, 1 (1979).
38. O. Parodi, *J. Phys. (Paris)*, **31**, 581 (1970).
39. M. Miesowicz, *Bull. Acad. Pol. Ser. A*, 228 (1936).
40. D. W. Berreman, in *Non-emissive Electro-optic Displays*, eds. A. R. Kmetz and F. K. von Willisen (Plenum, New York, 1976), p. 9.
41. C. Z. van Doorn, *J. Appl. Phys.*, **46**, 3738 (1975); D. W. Berreman, *J. Appl. Phys.*, **46**, 3746 (1975).
42. F. M. Leslie and C. M. Waters, *10th Internat. Liq. Cryst. Conf.* (York, UK, 1984), Paper C4.
43. J. Wahl and F. Fischer, *Mol. Cryst. Liq. Cryst.*, **22**, 359 (1973).
44. W. Zvetkow, *Acta Physicochim. URSS*, **10**, 555 (1939).
45. M. G. Clark, F. M. Leslie, F. C. Saunders and I. A. Shanks, *Mol. Cryst. Liq. Cryst.*, **70**, 195 (1981).
46. The observation in Reference 45 of imaginary θ_0 in 4-*n*-heptyl-4′-cyanobiphenyl (K21) has been disputed; see S. D. Hunnisett and J. C. A. van der Sluijs, *J. Phys. (Paris) Lett.*, **44**, L-59 (1983) and W. W. Beens and W. H. de Jeu, *J. Phys. (Paris) Lett.*, **44**, L-805 (1983).
47. M. G. Clark, F. M. Leslie and I. A. Shanks, British Patent no. 2042202 (1983); M. G. Clark and I. A. Shanks, *SID Internat. Symp. Digest*, **13**, 172 (1982).
48. F. Jähnig and F. Brochard, *J. Phys. (Paris)*, **35**, 301 (1974).
49. H. Kneppe, F. Schneider and N. K. Sharma, *Ber. Bunsenges Phys. Chem.*, **85**, 784 (1981); K. Sharp, T. Carlsson, S. T. Lagerwall and B. Stebler, *Mol. Cryst. Liq. Cryst.*, **66**, 199 (1981).
50. R. Y. Dong, *Mol. Cryst. Liq. Cryst.*, **72**, 59 (1981).
51. C. M. Waters, unpublished work.
52. J. Constant and E. P. Raynes, *Mol. Cryst. Liq. Cryst.*, **62**, 115 (1980).
53. A. E. White, P. E. Cladis and S. Torza, *Mol. Cryst. Liq. Cryst.*, **43**, 13 (1977).
54. S. Sarkar, *J. Phys. C: Solid State Phys.*, **15**, 6513 (1982); S. Sarkar, *Mol. Cryst. Liq. Cryst.*, **97**, 111 (1983).
55. J. H. Hildebrand, *Farad. Discuss. Chem. Soc.*, **66**, 151 (1978).
56. G. S. Grest and M. H. Cohen, *Advan. Chem. Phys.*, **48**, 455 (1981).
57. M. F. Bone, M. G. Clark and A. H. Price, to be published.